International Journal of Civil Engineering and Geo-Environmental

Journal homepage:http://ijceg.ump.edu.my
ISSN:21802742

QUASI-TWO-DIMENSIONAL DISCRETE VAPOUR CAVITY MODEL

ReyhanehNorooz[1*], Hamid Shamloo [2]

[1]PhD Student, Department of Civil Engineering, University of Tehran, Tehran 19697, Iran.
[2]Associate Professor, Department of Civil Engineering, K.N. Toosi University of Technology, Tehran 19697, Iran.

ARTICLEINFO

Keywords:
Pipelines
Water hammer
Column separation
Transient cavitating flow
Quasi-two-dimensional discrete vapour cavity model

A B S T R A C T

In the simulation of transient flow in hydraulic piping systems, vapourous cavitation occurs when thecalculated pressure head falls to the liquid vapour pressure head. Rapid valve closure or pump shutdown causes fast transient flow which results in large pressure variations, local cavity formation and distributed cavitation which potentially cause problems such as pipe failure, hydraulic equipment damage and corrosion. This paper presents a numerical study of water hammer with column separation in a simple reservoir-pipeline-valve system. In this study, as a new approach, water hammer with column separation has been modelled in a quasi-two-dimensional form. The governing equations for transient flow in pipes are solved based on the method of characteristics using a quasi-two-dimensional discrete vapour cavity model (quasi-two-dimensional DVCM)and a one-dimensional discrete vapour cavity model(one-dimensional DVCM). It was found that quasi-two-dimensional DVCM correlates better with the experimental data than one-dimensional DVCM in terms of pressure magnitude. The simulation results clearly show that proper selection of the number of computational reaches and the number of computational grids in radial direction in quasi-two-dimensional DVCM significantly improves the computational results.

1.0 Introduction

Concrete industry is one of the most important.Pipes are used to carry liquid reliably in water supply systems, irrigation networks and nuclear power plants. Hydraulic systems have a broad change of flow velocity which produces a pressure change. The rapid valve closure or pump failure causes fluid transients which produce large pressure change and cavitation. Cavitation can have a serious effect on the pumps, valves and other components performance. Therefore, it would be significant to predict the commencement and amount of cavitation occurring in order to improve the performance and reliability of systems. This will allow improving both pump and circuit design.

Vapourous cavitation occurs when the liquid pressure drops to the liquid vapour pressure. It may happen in two different types of cavitating flow: (1) a localized vapour cavity and (2) distributed vapourous cavitation. The first type has a large void fraction and happens at a boundary like closed valve or at a high point along the pipeline. The second type extends over long sections of the pipe. The void fraction for this type is small and close to zero and it happens when the pressure drops to the liquid vapour pressure over an extended region of the pipe. The collapse of large vapour cavity and the propagation of the shock wave through the vapourous cavitation zone cause the vapour change back to liquid. When vapour cavities change to liquid, large pressures with steep wave fronts may happen. As an outcome, fluid transients may lead to severe damages (Jaeger, 1948; Bonin, 1960; Parmakian, 1985; De Almeida, 1991).

Various types of vapourous cavitation models have been introduced (Wylie and Streeter, 1993; Bergant et al., 2006) including discrete cavity and interface

models. The discrete vapour cavity model (DVCM) (Wylie and Streeter, 1993; Wylie and Streeter, 1978) is the most popular model for column separation and distributed cavitation in recent years (Bergant et al., 2006). One positive point of the DVCM is that it is easily implemented and that it reproduces many features of column separation in pipelines (Bergant et al., 2006). The DVCM may produce unrealistic pressure pulses (spikes) due to the collapse of multi-cavities (Bergant et al., 2007), but there are some methods which reduce the unrealistic pressure pulses. Using quasi-two-dimensional DVCM or using unsteady friction model in one-dimensional DVCM reduces unrealistic pressure pulses.

In order to consider the DVCM in connection with transient flows, first it is needed to model the transient flow. Water hammer has been modelled by many researchers as either one-dimensional models or two-dimensional models. Although one-dimensional models are more popular, some important assumptions are ignored. For example, the velocity profile is assumed to be uniform in the cross section, but according to the no slip condition near the wall, the velocity should be considered zero. Therefore, two-dimensional models can be helpful to study some features which are not seen in one-dimensional models.

Quasi-two dimensional numerical model for turbulent water hammer flows has the attributes of being robust, consistent with the physics of wave motion and turbulent diffusion, and free from the inconsistency associated with the enforcement of the no slip condition while neglecting the radial velocity at boundary elements, such as valves and reservoirs (Zhao and Ghidaoui, 2003).

Quasi-two-dimensional governing equations form a system of hyperbolic–parabolic partial differential equations which cannot, in general, be solved analytically (Zhao and Ghidaoui, 2003). The numerical solution of Vardy and Hwang (1991) solves the hyperbolic part of the governing equations by the method of characteristics and the parabolic part by finite differences in a quasi-two-dimensional form. The solutions by Eichinger and Lein (1992) and Silva-Araya and Chaudhry (1997) solve the hyperbolic part of the governing equations by the method of characteristics in one-dimensional form and the parabolic part of the equations by finite differences in quasi-two-dimensional form. The solution by Pezzinga (1999) uses finite difference-based techniques to solve both hyperbolic part and parabolic part of the governing equations of turbulent flow in water hammer.

Practical implications of column separation led to intensive laboratory and field research starting at the end of 19th century (Joukowsky, 1900). Wylie and Streeter (1978, 1993) have described one-dimensional DVCM in detail. Researchers have attempted to incorporate a number of unsteady friction models into one-dimensional DVCM. Shuy and Apelt (1983) performed numerical analyses with a number of friction models including steady, quasi-steady and unsteady friction models. For the case of water hammer (no cavitation) they found little differences in the results of the models, but for the case with column-separation (two-phase flow) large discrepancies occurred. Brunone et al. (1991) used one-dimensional DVCM in combination with an instantaneous-acceleration unsteady friction model. Significant discrepancies between experiment and theory were found for all runs when using a quasi-steady friction term. Bergant and Simpson (1994) investigated the performance of quasi-steady and unsteady friction models similar to those used by Shuy and Apelt (1983). The instantaneous-acceleration and convolution-based unsteady friction models gave the best fit with experimental data for the case of water hammer. Bughazem and Anderson (2000) developed one-dimensional DVCM with an instantaneous-acceleration unsteady friction term and found good agreement between theory and experiment. Numerical studies by Bergant and Tijsseling (2001) have shown that unsteady friction may cause a significant damping of the pressure spikes observed in measurements.

In this study, as a new approach, water hammer with column separation has been modelled in a quasi-two-dimensional form. The results and the efficiency of quasi-two-dimensional modeling have been compared with one-dimensional modeling. First, the structure of one-dimensional DVCM and quasi-two-dimensional DVCM are explained and then the DVCM is considered to study the column separation in a reservoir-pipeline-valve system. The numerical model of Vardy and Hwang (1991) is chosen for quasi-two-dimensional DVCM. They used the method of characteristics in longitudinal direction and finite-difference discretization in radial direction which makes it suitable to study the physics of the flow.

2.0 One-dimensional Discrete VapourCavity Model

When the pressure is more than the liquid vapour pressure, transient flow in pipelines is described by one-dimensional equations of continuity and motion(Wylie and Streeter, 1993):

$$\frac{\partial Q}{\partial t} + gA\frac{\partial H}{\partial x} + \frac{fQ|Q|}{2DA} = 0 \quad (1)$$

$$c^2\frac{\partial Q}{\partial x} + gA\frac{\partial H}{\partial t} = 0 \quad (2)$$

where$x$ = distance along the pipe, ρ = density of liquid, c = liquid (elastic) wave speed, t = time, f = Darcy-Weisbach friction factor, D = internal pipe diameter, g = gravitational acceleration,Q = discharge, H = pressure head and A = cross-sectional flow area.

The method of characteristics is a standard method for solving the unsteady-flow equations. The method of characteristics transformation of the equations gives the compatibility equations which are valid along the characteristics lines (Wylie and Streeter, 1993). The compatibility equations, written in a finite-difference form for the i-th computational sectionwithin the staggered (diamond) grid are (Wylie and Streeter, 1993).

- along the C^+ characteristic line ($\Delta x/\Delta t=c$):

$$H_i^n - H_{i-1}^{n-1} + \frac{c}{gA}\left(Q_i^{n,u} - Q_{i-1}^{n-1,d}\right) + \frac{f\Delta x}{2gDA^2}Q_i^{n,u}\left|Q_{i-1}^{n-1,d}\right| = 0 \quad (3)$$

- along the C^- characteristic line ($\Delta x/\Delta t = -c$):

$$H_i^n - H_{i+1}^{n-1} - \frac{c}{gA}\left(Q_i^{n,d} - Q_{i+1}^{n-1,u}\right) - \frac{f\Delta x}{2gDA^2}Q_i^{n,d}\left|Q_{i+1}^{n-1,u}\right| = 0 \quad (4)$$

whereQ^u and Q^d are the upstream and downstream discharge respectively which are introduced to accommodate the DVCM. They are equal for the case of no column separation. If the pressure falls to the liquid vapour pressure, column separation happens either as a discrete cavity or a vapourous cavitation zone (Simpson, 1986; Simpson and Wylie, 1991) in the liquid.

In the DVCM, cavities are allowed to form at the computational sections if the computed pressure becomes less than the liquid vapour pressure. However, the DVCM does not differentiate between localized vapour cavities and distributed vaporous cavitation (Simpson and Wylie, 1989; Bergant and Simpson, 1999). The classical water hammer solution is no longer valid at a vapour pressure section. To solve the compatibility equations at a vapour pressure section, the head is set equal to the vapour pressure head H_{vap}. Pure liquid with a constant wave speed c is assumed to occupy between computational sections. Then the continuity equation for cavity volume $\forall_{vap}$ is expressed as (Wylie, 1984):

$$\forall_{vap}{}_i^n = \forall_{vap}{}_i^{n-2} + \left(1-\psi\right)\left(Q_i^{n-2,d} - Q_i^{n-2,u}\right) + \psi\left(Q_i^{n,d} - Q_i^{n,u}\right)2\Delta t \quad (5)$$

whereψ = weighting factor and takes values between 0 and 1.0. The cavity collapses when its calculated volume becomes negative and the one-phase liquid flow is re-established so that the water hammer solution using Equations (3) and (4) (with ($Q_i^{n,u} \equiv Q_i^{n,d}$) is valid again.

3.0 Friction Model

The friction term in one-dimensional transient flow is expressed as the sum of the unsteady part f_u and the quasi-steady partf_q:

$$f = f_q + f_u \quad (6)$$

There are several friction models which have been introduced by many researchers to consider the unsteady part. The Brunone model(Brunone et al., 1991), which is based on mean flow velocity and local acceleration, has special popularity because of its simplicity and accuracy.

This model was improved by Vitkovsky in 1998 to predict a correct sign of the convective term in the case of closure of the upstream end valve in a simple pipeline system with the initial flow in the positive x direction (Bergant and Simpson, 1994; Brunone et al., 1995):

$$f_u = \frac{kD}{V|V|}\left[\frac{\partial V}{\partial t} + csign\left(V\right)\left|\frac{\partial V}{\partial x}\right|\right] \quad (7)$$

where, k is the Brunone's friction coefficient and x is the distance along the pipe and sign(V) = (+1 for $V\geq 0$ or -1 for $V< 0$). Vardy and Brown proposed the following empirical relationship to derive the Brunone coefficient analytically (Bergant et al., 2001; Vardy and Brown, 1996):

$$k = \frac{\sqrt{C^*}}{2} \quad (8)$$

The Vardy shear decay coefficient C^* from Vardy and Brown (1996) is:

- laminar flow:

$$C^* = 0.00476 \quad (9)$$

- turbulent flow:

$$C^* = \frac{7.41}{\mathrm{Re}^{\log 14.3/\mathrm{R}^{0.05}}} \qquad (10)$$

in which Re = Reynolds number (Re = VD/υ).

4.0 Quasi –Two-dimensional Discrete Vapour Cavity Model

Quasi-two-dimensional continuity and motion equations for an elastic pipe with circular cross section are defined as(Vardyand Hwang, 1991):

$$\frac{g}{c^2}\frac{\partial H}{\partial t} + \frac{\partial u}{\partial x} + \frac{1}{r}\frac{\partial rv}{\partial r} = 0 \qquad (11)$$

$$\frac{\partial u}{\partial t} + g\frac{\partial H}{\partial x} = \frac{1}{r\rho}\frac{\partial r\tau}{\partial r} \qquad (12)$$

where$x$ = distance along the pipe, r = distance from the axis in radial direction, t = time, H = pressure head, u = local longitudinal velocity, v = local radial velocity, g = gravitational acceleration, c = liquid (elastic) wave speed; ρ = density of liquid and τ = shear stress.

Numerical solutions are used to approximate the hyperbolic–parabolic partial differential equations. The numerical solution of Vardy and Hwang (1991) solves the hyperbolic part of the governing equations by the method of characteristics and the parabolic part by finite differences in a quasi-two-dimensional form.
The shear stress τ can be expressed as:

$$\tau = \rho\upsilon\frac{\partial u}{\partial r} - \rho\overline{u'v'} \qquad (13)$$

whereυ = kinematic viscosity, u□, v□ = turbulence fluctuations corresponding to longitudinal velocity u, and radial velocity v respectively. Turbulence models are needed to solve the Reynolds stress term $\rho\overline{u'v'}$.
According to the Boussinesq approximation, the turbulent shear stress is given by:

$$-\rho\overline{u'v'} = \rho\upsilon_t\frac{\partial u}{\partial r} \qquad (14)$$

where, υ_t is eddy viscosity.

The grid system is shown in Fig. The pipe is discretized into N_r cylinders with constant area ΔA in radial direction. The wall thickness of the mth cylinder is denoted by Δr_m, where $m = 1,\ldots,j,\ldots,N_r$ and $\Delta r_m = r_m - r_{m-1}$. The pipe length, L, is divided into N_x equal reaches such that $\Delta x = L/N_x$. The time step is determined by $\Delta t = \Delta x/c$(i.e., Courant number $C_r = 1.0$).

Using the grid shown in Fig, integrating along the positive and negative characteristics gives:

$$H_i^{n+1} - \theta C_{q1}\ j\ q_{i,j-1}^{n+1} + \theta C_{q2}\ j\ q_{i,j}^{n+1} - \varepsilon C_{u1}\ j\ u_{i,j-1}^{n+1,u} + \left[\frac{c}{g} + \varepsilon C_{u2}\ j\right] u_{i,j}^{n+1,u}$$
$$- \varepsilon C_{u3}\ j\ u_{i,j+1}^{n+1,u} = H_{i-1}^{n} + (1-\theta)\ C_{q1}\ j\ q_{i-1,j-1}^{n} - (1-\theta)\ C_{q2}\ j\ q_{i-1,j}^{n}$$
$$+ (1-\varepsilon)\ C_{u1}\ j\ u_{i-1,j-1}^{n,d} + \left[\frac{c}{g} - (1-\varepsilon)\ C_{u2}\ j\right] u_{i-1,j}^{n,d} + (1-\varepsilon)\ C_{u3}\ j\ u_{i-1,j+1}^{n,d} \qquad (15)$$

$$H_i^{n+1} - \theta C_{q1}\ j\ q_{i,j-1}^{n+1} + \theta C_{q2}\ j\ q_{i,j}^{n+1} + \varepsilon C_{u1}\ j\ u_{i,j-1}^{n+1,d} - \left[\frac{c}{g} + \varepsilon C_{u2}\ j\right] u_{i,j}^{n+1,d}$$
$$+ \varepsilon C_{u3}\ j\ u_{i,j+1}^{n+1,d} = H_{i+1}^{n} + (1-\theta)\ C_{q1}\ j\ q_{i+1,j-1}^{n} - (1-\theta)\ C_{q2}\ j\ q_{i+1,j}^{n}$$
$$- (1-\varepsilon)\ C_{u1}\ j\ u_{i+1,j-1}^{n,u} - \left[\frac{c}{g} - (1-\varepsilon)\ C_{u2}\ j\right] u_{i+1,j}^{n,u} - (1-\varepsilon)\ C_{u3}\ j\ u_{i+1,j+1}^{n,u} \qquad (16)$$

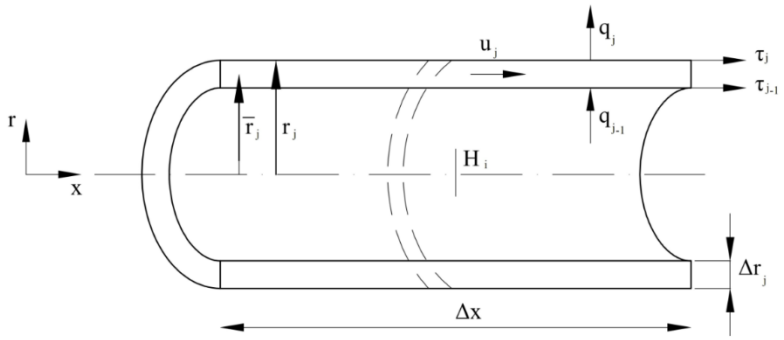

Figure 1: Grid system for numerical solution

where u_i^u and u_i^d are the upstream and downstream longitudinal velocity, respectively which have been introduced to accommodate the DVCM. They are equivalent for the classical water hammer. θ, ε = weighting coefficients; subscript *i*, *j* and superscript *n* indicate the spatial and temporal locations, respectively, of the grid point with coordinate ($i\Delta x$, r_j, $n\Delta t$); Δt = time step; $r_j = \sum_{m=1}^{j} \Delta r_m$; and $\overline{r_j} = r_{j-1} + r_j \ / 2$ such that $r_0 = 0$. The coefficients in Equations (15)and(16) are as follows:

$$C_{q1} \ \ j \ = C_{q2} \ \ j \ = \frac{c^2 \Delta t}{g} \frac{1}{\overline{r_j} \Delta r_j}$$

$$C_{u1} \ \ j \ = \frac{c \Delta t \upsilon_{T_{j-1}}}{g} \frac{1}{\overline{r_j} \Delta r_j} \frac{r_{j-1}}{\overline{r_j} - \overline{r_{j-1}}}$$

$$C_{u3} \ \ j \ = \frac{c \Delta t \upsilon_{T_j}}{g} \frac{1}{\overline{r_j} \Delta r_j} \frac{r_j}{\overline{r_{j+1}} - \overline{r_j}}$$

$$C_{u2} \ \ j \ = C_{u1} \ \ j \ + C_{u3} \ \ j$$

where υ_T =total viscosity.

When the computed head is more than the liquid vapour pressure at a given location along the pipe *i*, there are two equations for each cylinder, namely Equations(15) and (16). Since there are N_r cylinders in total, the number of equations is $2N_r$. Therefore, the governing equations at (i,n+1) for all j (i.e., for all cylinders) can be written in matrix form as follows: **Az**=**b**, where **A**=a$2N_r \times 2N_r$ matrix which its form is as follows:

$$
\begin{pmatrix}
1 & \frac{c}{g}+\varepsilon C_{u2}\ 1 & \theta C_{q2}\ 1 & -\varepsilon C_{u3}\ 1 & & & \\
1 & -\left[\frac{c}{g}+\varepsilon C_{u2}\ 1\right] & \theta C_{q2}\ 1 & \varepsilon C_{u3}\ 1 & & & \\
 & . & & . & & . & \\
 & . & & . & & . & \\
 & . & & . & & . & \\
1 & \ldots & -\varepsilon C_{u1}\ j & -\theta C_{q1}\ j & \frac{c}{g}+\varepsilon C_{u2}\ j & \theta C_{q2}\ j & -\varepsilon C_{u3}\ j \ldots \\
1 & \ldots & \varepsilon C_{u1}\ j & -\theta C_{q1}\ j & -\left[\frac{c}{g}+\varepsilon C_{u2}\ j\right] & \theta C_{q2}\ j & \varepsilon C_{u3}\ j \ldots \\
 & & & . & & . & \\
 & & & . & & . & \\
 & & & . & & . & \\
1 & & & & -\varepsilon C_{u1}\ Nr & -\theta C_{q1}\ Nr & \frac{c}{g}+\varepsilon C_{u2}\ Nr \\
1 & & & & \varepsilon C_{u1}\ Nr & -\theta C_{q1}\ Nr & -\left[\frac{c}{g}+\varepsilon C_{u2}\ Nr\right]
\end{pmatrix}
$$

$\mathbf{z}= \left(H_i^{n+1}, u_{i,1}^{n+1}, q_{i,1}^{n+1}, \ldots, u_{i,j}^{n+1}, q_{i,j}^{n+1}, \ldots, u_{i,Nr-1}^{n+1}, q_{i,Nr-1}^{n+1}, u_{i,Nr}^{n+1}\right)^T$ =unknown vector; superscript T denotes the transpose operator; and **b**=known vector which depends on head and velocities at time level n. Therefore, the solution for head, and longitudinal as well as radial velocities at (i , n+1) for all j involves the inversion of a $2N_r \times 2N_r$ Modified Vardy–Hwang Scheme matrix.

When computed head falls to the liquid vapor pressure, the classical water hammer solution is no longer valid at a vapor pressure section. The head at this section is set to the liquid vapor pressure head and it is needed to solve the compatibility equations separately. Local radial velocity is neglected. Therefore, along the positive line of characteristics method, the governing equations at (i , n+1) for all j (i.e., for all cylinders) can be written in matrix form as follows: $\mathbf{Bu}=\mathbf{b_u}$, where $\mathbf{B}=aN_r \times N_r$ matrix which its form is as follows:

$$\begin{pmatrix} \left[\frac{c}{g}+\varepsilon C_{u2}\ \ 1\right] & -\varepsilon C_{u3}\ \ 1 & & & \\ & \cdot & & \cdot & \\ & \cdot & & \cdot & \\ & \cdot & & \cdot & \\ \ldots & -\varepsilon C_{u1}\ \ j & \left[\frac{c}{g}+\varepsilon C_{u2}\ \ j\right] & -\varepsilon C_{u3}\ \ j & \ldots \\ & \cdot & & \cdot & \\ & \cdot & & \cdot & \\ & \cdot & & \cdot & \\ & & & -\varepsilon C_{u1}\ \ Nr & \left[\frac{c}{g}+\varepsilon C_{u2}\ \ Nr\right] \end{pmatrix}$$

$\mathbf{u}= \left(u_{i,1}^{n+1,u},\ldots,u_{i,j}^{n+1,u},\ldots,u_{i,Nr-1}^{n+1,u},u_{i,Nr}^{n+1,u}\right)^T$=unknown vector; superscript T denotes the transpose operator; and $\mathbf{b_u}$=known vector which depends on head and velocities at time level n. Therefore, the solution for head, and longitudinal velocities at (i , n+1) for all j at the upstream sides in the involves the inversion of $aN_r \times N_r$ Modified Vardy–Hwang Scheme matrix. For computing longitudinal velocity at the downstream sides of the computational section, it is needed to solve $\mathbf{Cd=b_d}$ along the negative line of characteristics method. $\mathbf{C}=aN_r \times N_r$ matrix is written as follows:

$$\begin{pmatrix} -\left[\frac{c}{g}+\varepsilon C_{u2}\ \ 1\right] & \varepsilon C_{u3}\ \ 1 & & & \\ & \cdot & & \cdot & \\ & \cdot & & \cdot & \\ & \cdot & & \cdot & \\ \ldots & \varepsilon C_{u1}\ \ j & -\left[\frac{c}{g}+\varepsilon C_{u2}\ \ j\right] & \varepsilon C_{u3}\ \ j & \ldots \\ & \cdot & & \cdot & \\ & \cdot & & \cdot & \\ & \cdot & & \cdot & \\ & & & \varepsilon C_{u1}\ \ Nr & -\left[\frac{c}{g}+\varepsilon C_{u2}\ \ Nr\right] \end{pmatrix}$$

$\mathbf{b_d}= \left(u_{i,1}^{n+1,d},\ldots,u_{i,j}^{n+1,d},\ldots,u_{i,Nr-1}^{n+1,d},u_{i,Nr}^{n+1,d}\right)^T$ unknown vector; superscript T denotes the transpose operator; and $\mathbf{b_d}$=known vector which depends on head and velocities at time level n. Therefore, the solution for head, and longitudinal velocities at (i , n+1) for all j at the downstream sides in the involves the inversion of a $N_r \times N_r$ Modified Vardy–Hwang Scheme matrix. In the quasi-two-dimensional DVCM, the continuity equation for cavity volume is similar to one-dimensional DVCM (Equation(5)).

5.0 Five-Region-Turbulence Model

The five-region turbulence model is presented by Kita et al. (1980). In this model the steady-state eddy viscosity distribution is divided into five different regions, namely the viscous layer, the buffer I and II layers, the logarithmic region and the core region. The distributions of the eddy viscosity and intervals of the different regions are as follows (Kita et al., 1980):

Viscous layer: $\upsilon_t = \upsilon, 0 \le y_* \le \frac{1}{C_a}$

Buffer I layer: $\upsilon_t = C_a y_* \upsilon, \frac{1}{C_a} \le y_* \le \frac{C_a}{C_b}$

Buffer II layer:

$$\upsilon_t = \upsilon C_b {y_*}^2, \frac{C_a}{C_b} \le y_* \le \frac{\kappa}{C_b + \kappa^2 / 4C_m R_*}$$

Logarithmic region:

$$\upsilon_t = \upsilon C_c y_* \left(1 - \frac{\kappa y_*}{4C_m R_*}\right), \frac{\kappa}{C_b + \kappa^2 / 4C_m R_*} \le y_* \le \frac{2C_m}{\kappa}\left(1 + \sqrt{1 - C_c / C_m}\right) R_*$$

Core region:

$$\upsilon_t = \upsilon C_c R_*, \frac{2C_m}{\kappa}\left(1 + \sqrt{1 - C_c / C_m}\right) R_* \le y_* \le R_*$$

Here the constants and variables are defined as:

$$y_* = \frac{u_* y}{\upsilon}, R_* = \frac{u_* R}{\upsilon}, u_* = \sqrt{\tau_w}, C_a = 0.19, C_b = 0.011, \kappa = 0.37, C_m = 0.077$$

where τ_w is the wall shear stress, the variable y_* is the dimensionless wall distance, the constant R_* is the dimensionless pipe radius and u_* is the frictional velocity. The constant κ is the von Karman's constant and the variable C_c is defined as:

$$C_c = \begin{cases} 0.07, & \mathrm{R} < 10^4 \\ 0.4095 - 0.1390\ln(\mathrm{Re}) + 0.0137\ln(\mathrm{Re})^2, & 10^4 \le \mathrm{R} \le 10^6 \\ 0.075, & \mathrm{R} > 10^6 \end{cases}$$

6.0 Experimental Apparatus

The computational results are compared with the results of experimental studies conducted by Bergant and Simpson (1995) which were carried out using a long horizontal pipe with length of 37.20 m and inner diameter of 0.0221 m that connects upstream and downstream reservoirs (see Fig). The water hammer wave speed was experimentally determined as c = 1319 m/s. A transient event is initiated by a rapid closure of the ball valve.

Five pressure transducers are mounted at equidistant points along the pipeline including as close as possible to the reservoirs. Pressures measured at the valve (H_v) and at the midpoint (H_{mp}) are presented in this paper. The uncertainties in the measurements are fully described by Bergant and Simpson (1995).

7.0 Comparison of Numerical Models

In order to investigate the performance of quasi-two-dimensional DVCM and one-dimensional DVCM and the effects of mesh size on accuracy of the results, the numerical and experimental results were compared in three runs. Computational runs were performed for a rapid closure of the valve positioned at the downstream end of the horizontal pipe at the downstream reservoir (see Fig). The initial velocity was V_0= 0.3 m/s and the constant static head in the upstream reservoir and the vapour pressure head were H_{ur}= 22 m and H_{vap}= -10.25 m. The initial Reynolds number was 5970 and the rapid valve closure began at time t = 0 s. The weighting factor ψ in Equation (5) was chosen as 1.0 in all three runs. To study the effects of mesh size, various numbers of reaches were selected, N_x= {32, 128, 202} for quasi-two-dimensional DVCM and one-dimensional DVCM and different numbers of computational grids in radial direction, N_r= {20, 40, 50} were selected for quasi-two-dimensional DVCM.

Rapid valve closure for the discussed low-initial flow velocity case generates a water hammer event with moderate cavitation. The location and intensity of discrete vapour cavities is governed by the type of transient regime, layout of the piping system and hydraulic characteristics (Bergant and Simpson, 1999). The maximum head at the valve which has been measured in the lab, is 96.6 m and it occurred 0.18 s after valve closure.

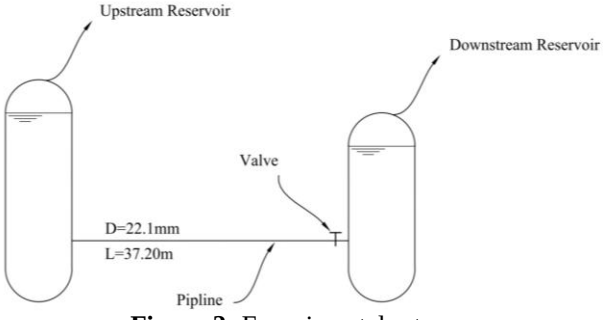

Figure 2: Experimental set up

The computational results for the first run with the number of computational reaches N_x= 32 for quasi-two-dimensional DVCM and one-dimensional DVCM and the number of computational grids in the radial direction N_r = 20 for quasi-two-dimensional DVCM are presented in Fig. Fig agrees well till 0.22 s. The discrepancies between the results are magnified later times. The maximum computed heads predicted by quasi-two-dimensional DVCM and one-dimensional DVCM are:

(1) Quasi-two-dimensional DVCM: $H_{v,max}$= {N_x= 32, N_r = 20, ψ = 1, 111.588 m at t = 0.169 s}

(2) One-dimensional DVCM: $H_{v,max}$= {N_x= 32, ψ = 1, 110.53 m at t = 0.173 s}

Both quasi-two-dimensional DVCM and one-dimensional DVCM slightly overestimate the maximum heads. According to Fig, one-dimensional DVCM yields better conformance with the experimental data while quasi-two-dimensional DVCM yields poor results, and gives a better timing of the transient event than quasi-two-dimensional DVCM.

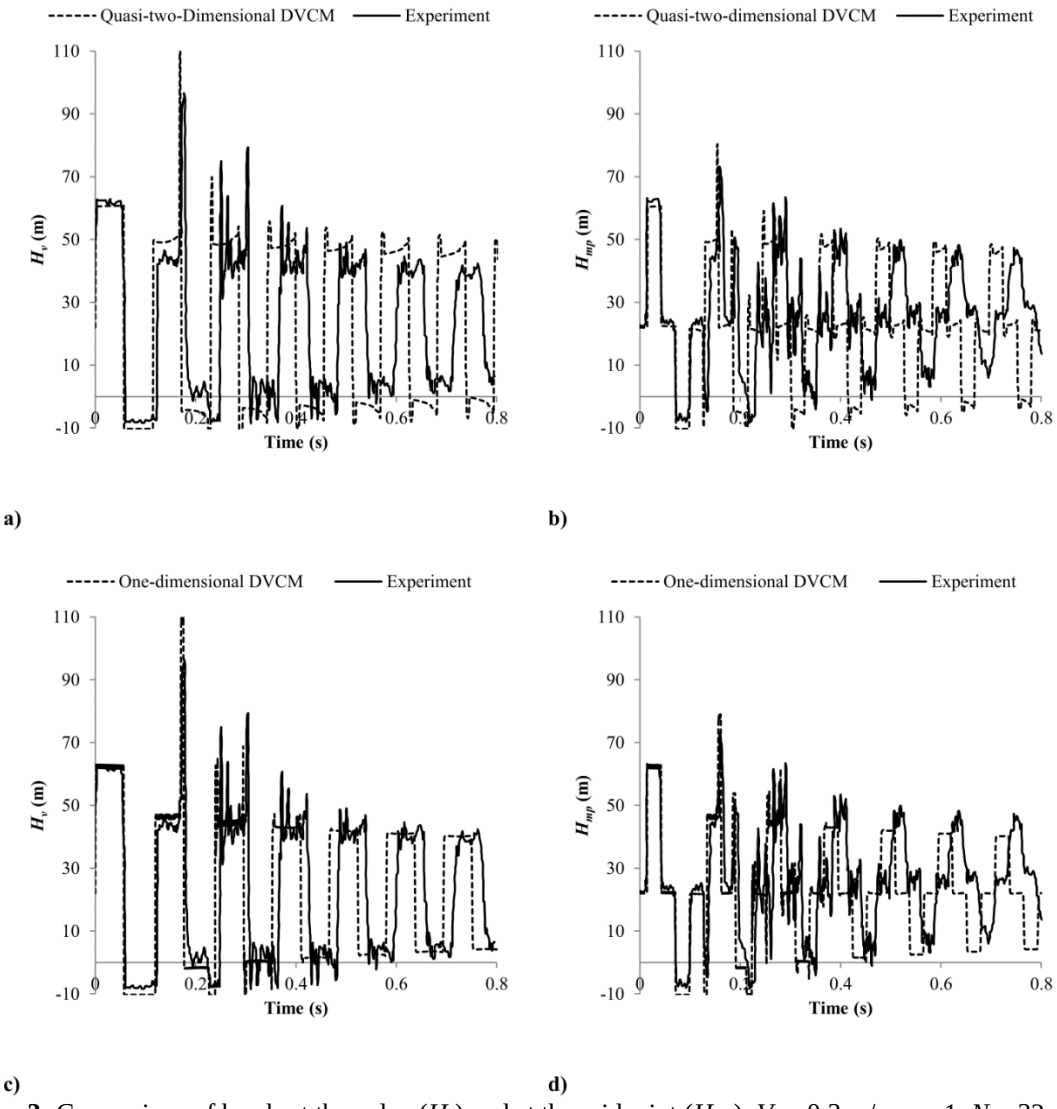

Figure 3: Comparison of heads at the valve (H_v) and at the midpoint (H_{mp}): V_0 = 0.3 m/s, ψ = 1, N_x= 32 and N_r= 20

The results of the second and third runs are presented in Figures 4 and 5 respectively. It should be noted that in the second run the number of longitudinal reaches was 128 and the radial ones was 40, and in the third run these parameters were considered 202 and 50 respectively.

Figures 4 and 5 agree well till 0.22 s, and the discrepancies between the numerical and experimental

results are magnified as time increases. The maximum computed heads predicted by quasi-two-dimensional DVCM and one-dimensional DVCM are:

In the second run:

(1) Quasi-two-dimensional DVCM: $H_{v,max}$= {N_x= 128, N_r = 40, ψ = 1, 109.30 m at t = 0.172 s}
(2) One-dimensional DVCM: $H_{v,max}$= {N_x= 128, ψ = 1, 110.31 m at t = 0.175 s}

In the third run:

(1) Quasi-two-dimensional DVCM: $H_{v,max}$= {N_x= 202, N_r = 50, ψ = 1, 108.55 m at t = 0.172 s}
(2) One-dimensional DVCM: $H_{v,max}$= {N_x= 202, ψ = 1, 110.19 m at t = 0.175 s}

In both runs, both quasi-two-dimensional DVCM and one-dimensional DVCM slightly overestimate the maximum heads. In the second run (

Fig), the quasi-two-dimensional DVCM has become more successful to predict the maximum head, the same result is also seen in the third run (Fig), but still one-dimensional DVCM has better agreement in terms of simulating the time of the maximum head in both second and third runs.

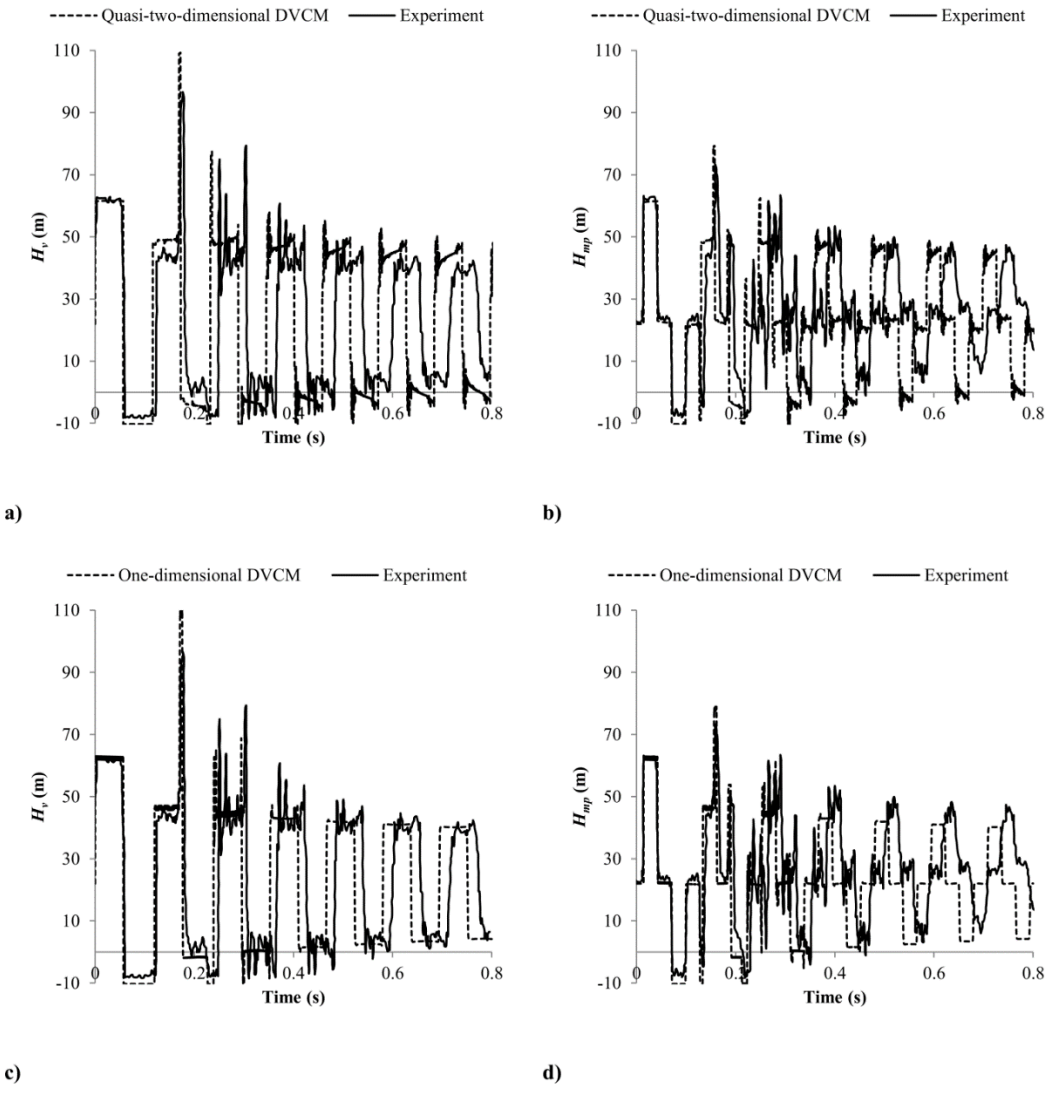

Figure 4: Comparison of heads at the valve (H_v) and at the midpoint (H_{mp}): V_0 = 0.3 m/s, ψ = 1, N_x= 128 and N_r= 40

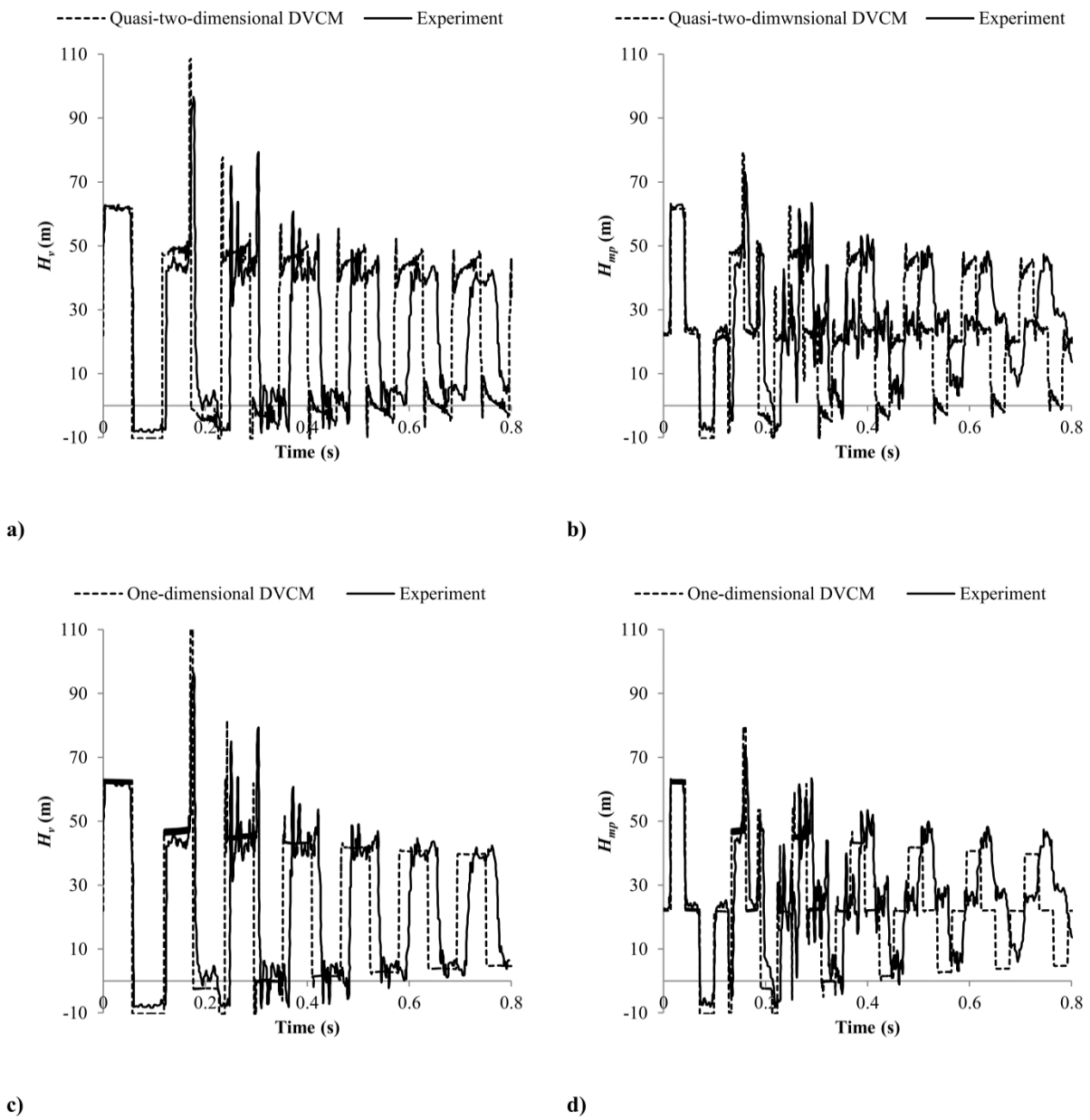

Figure 5: Comparison of heads at the valve (H_v) and at the midpoint (H_{mp}): V_0= 0.3 m/s, ψ = 1, N_x= 202 and N_r= 50

In these two models, unrealistic pressure pulses do not exist and generally, quasi-two-dimensional DVCM exhibits a capability to reproduce the experimental oscillations while one-dimensional DVCM disregards them and just reproduces them with sufficient accuracy in a short time immediately after closing the valve (Figures 3, 4 and 5). Results obtained by one-dimensional DVCM show strong attenuation of the main pressure pulses at later times (see Figures 3, 4 and 5). It is worth noting that one-dimensional DVCM produces less phase shift than quasi-two-dimensional DVCM even in the finest mesh.

The influence of different numbers of reaches (N_x) for quasi-two-dimensional DVCM and one-dimensional DVCM and the influence of different numbers of computational grids in radial direction (N_r) for quasi-two-dimensional DVCM were investigated. Examination of computational results reveals numerically stable behavior of the models.

Apparently, when the number of reaches (N_x) and the number of computational grids in radial direction (N_r) are larger, quasi-two-dimensional DVCM gives better results when it comes to the maximum heads and timing of the transient event and it gives a better

prediction of the oscillations which exist in the experimental results.

In the first run with the coarsest mesh, the maximum volume of the cavity at the valve predicted by one-dimensional DVCM and quasi-two-dimensional DVCM is about 1.05×10^{-6} m^3 and 0.53×10^{-6} m^3 respectively (0.24 % of the reach volume for one-dimensional DVCM and 0.12 % of the reach volume for quasi-two-dimensional DVCM). In the second run, the maximum volume of the cavity at the valve predicted by one-dimensional DVCM and quasi-two-dimensional DVCM equals to about 0.96×10^{-6} m^3 and 0.54×10^{-6} m^3 respectively (0.87 % of the reach volume for one-dimensional DVCM and 0.49 % of the reach volume for quasi-two-dimensional DVCM). Finally, the values are about 0.93×10^{-6} m^3 in quasi-two-dimensional DVCM and 0.54×10^{-6} m^3 in one-dimensional DVCM (1.33 % of the reach volume for one-dimensional DVCM and 0.7 % of the reach volume for quasi-two-dimensional DVCM).

Careful examination of quasi-two-dimensional DVCM and one-dimensional DVCM reveals that one-dimensional DVCM produces more intense cavitation along the pipe than quasi-two-dimensional DVCM. The discrepancies between the computed results found by time-history comparisons may be attributed to the intensity of cavitation along the pipeline (distributed vapourous cavitation regions, actual number and position of intermediate cavities) resulting in a slightly different timing of cavity collapse and consequently a different superposition of waves.

8.0 Conclusion

Column separation occurs when the liquid pressure decreases to the liquid vapour pressure. When vapour cavities change to liquid, large pressures with steep wave fronts may happen. The DVCM is the most popular model for column separation and distributed cavitation in recent years. Unrealistic pressure pulses (spikes) in the DVCM due to the collapse of multi-cavities can be reduced by using quasi-two-dimensional DVCM or using unsteady friction model in one-dimensional DVCM.

In this study, as a new approach, transient flow with column separation has been modelled in quasi-two-dimensional form. In comparison of quasi-two-dimensional with one-dimensional models, the following results were deduced:

- Quasi-two-dimensional DVCM is better at simulating the oscillations which exist in the experimental results while one-dimensional DVCM does not show these oscillations.
- Quasi-two-dimensional DVCM corresponds with sufficient accuracy to the experimental data and predicts the maximum heads very well for large number of reaches (N_x) and computational grids in radial direction (N_r).
- There are not unrealistic pressure pulses in quasi-two-dimensional DVCM and one-dimensional DVCM which are one of the drawbacks of the DVCM.
- One-dimensional DVCM estimates the cavity volume larger than quasi-two-dimensional DVCM.
- One-dimensional DVCM produces less phase shift than two-dimensional DVCM even in the finest mesh.

List of symbols

$\mathbf{A}$	system matrix
A	cross-sectional flow area
$\mathbf{B}$	matrix for subsystem of longitudinal velocity component at the upstream of the computational section
$\mathbf{b}$	known vector for system
$\mathbf{b_d}$	known vector for subsystem of longitudinal velocity at the downstream of the computational section
$\mathbf{b_u}$	known vector for subsystem of longitudinal velocity at the upstream of the computational section
$\mathbf{C}$	matrix for subsystem of head and longitudinal velocity component at the downstream of the computational section
C_a, C_b, C_c, C_m	coefficients for five-region turbulence model
C_{q1}, C_{q2}	coefficients before q in quasi-two-dimensional DVCM
C_r	courant number
C_{u1}, C_{u2}, C_{u3}	coefficients before u in quasi-two-dimensional DVCM
C^*	Vardy's shear decay coefficient
c	liquid wave speed
D	internal pipe diameter
$\mathbf{d}$	unknown vector for subsystem of head and longitudinal velocity component at the downstream side of the computational section
E	Young's modulus of elasticity of pipe material
e	thickness of pipe wall
f	Darcy-Weisbach friction factor
f_q	quasi-steady friction
f_u	unsteady friction
g	gravitational acceleration
H	pressure head

$H_{v,max}$ maximum piezometric head at the valve
H_{mp} piezometric head at the midpoint
H_{ur} upstream reservoir head
H_v piezometric head at the valve
H_{vap} vapour pressure head
i index for computational section
j index for computational grids in radial direction
k Brunone's friction coefficient
L pipe length
N_r number of computational grids in radial direction
N_x numbers of reaches
n index for t
Q discharge
Q^d downstream discharge
Q^u upstream discharge
q radial flux
R radius of pipe
Re Reynolds number
R_* dimensionless pipe radius
r distance from the axis in radial direction
r_j radial coordinate for shear stress τ_j
$\overline{r_j}$ radial coordinate for velocity u_j
t time
u local longitudinal velocity
u unknown vector for subsystem of longitudinal velocity component at the upstream side of the computational section
u^d downstream local longitudinal velocity
u^u upstream local longitudinal velocity
u_* frictional velocity
u□ turbulence perturbation corresponding to longitudinal velocity
V average velocity
V_0 initial velocity
v local radial velocity
v□ turbulence perturbation corresponding to radial velocity
x distance along the pipe
y radial distance from wall
y_* dimensionless wall distance
z unknown vector for system
Δr_j incremental element associate to velocity u_j
Δt time steph
Δx reach length
ε implicit parameter for shear stress
κ coefficient for five-region turbulence model
θ implicit parameter for radial flux
υ kinematic viscosity
υ_T total viscosity
υ_t eddy viscosity
ρ density of liquid
τ shear stress
τ_w wall shear stress
ψ weighting factor
$\forall_{vap}$ discrete vapour cavity volume; and
DVCM discrete vapour cavity model

References

Bergant, A. and Simpson, A.R. (1994) Estimating unsteady friction in transient cavitating pipe flow. *Water pipeline systems*, D.S. Miller, ed., Mechanical Engineering Publications, London, 3-16.

Bergant, A. and Simpson, A.R. (1995) Water hammer and column separation measurements in an experimental apparatus. *Res. Rep. No. R128*, Dept. of Civ. and Envir. Engrg., The University of Adelaide, Adelaide, Australia.

Bergant, A. and Simpson, A.R. (1999) Pipeline column separation flow regimes. *Journal of HydraulicEngineering*, ASCE, 125, 835 - 848.

Bergant, A. andTijsseling, A.S. (2001) Parameters affecting water hammer wave attenuation, shape and timing. *Proc., 10th Int. Meeting of the IAHR Work Group on the Behaviour of Hydraulic Machinery under Steady Oscillatory Conditions (Eds. Brekke, H., Kjeldsen, M.)*, Trondheim, Norway, Paper C2, 12.

Bergant, A., Simpson, A.R., andTijsseling, A.S. (2006) Water hammer with column separation: a historical review. *Journal of Fluids and Structures*, 22(2), 135-171.

Bergant, A., Simpson, A.R. andVitkovsky , J. (2001) Developments in unsteady pipe flow friction modelling. *Journal of Hydraulic Research*, IAHR, 39(3), 249–257.

Bergant, A., Tijsseling, A.S., Vitkovsky, J., Simpson, A.R. and Lambert, M. (2007) Discrete Vapour Cavity Model with Improved Timing of Opening and Collapse of Cavities. *Proc.,2nd Int. Meeting of the IAHR Work Group on Cavitation and Dynamic Problems in Hydraulic Machinery and Systems.*

Bonin, C.C. (1960) Water-hammer damage to Oigawa Power Station. *Journal ofEngineering for Power*, ASME,82, 111-119.

Brunone, B.,Golia, U.M. and Greco, M. (1991)Some remarks on the momentum equation for fast transients. *Pro., 9th Int. Meeting of the IAHR Work Group on Hydraulic Transients with ColuSeparation (Eds. Cabrera, E., Fanelli, M.A.)*, Valencia, Spain, 140-148.

Brunone, B., Golia, U.M., and Greco, M. (1995) Effects of two-dimensionality on pipe transients

modelling. *Journal of Hydraulic Engineering*, ASCE, 121(12), 906-912.

Bughazem, M.B. and Anderson, A. (2000) Investigation of an unsteady friction model for water hammer and column separation. In: Anderson, A. (Ed.), Pressure Surges. Safe design and operation of industrial pipe systems, Professional Engineering Publishing Ltd., Bury St. Edmunds, UK, 483-498.

De Almeida, A.B. (1991) Accidents and incidents: A harmful/powerful way to develop expertise on pressure transients. *Pro.*, 9th *Int. Meeting of the IAHR Work Group on Hydraulic Transients with Column Separation (Eds. Cabrera, E., Fanelli, M.A.)*, Valencia, Spain, 379-401.

Eichinger, P. andLein, G. (1992)The influence of friction on unsteady pipe flow. *Unsteady flow and fluid transients*, Bettess and Watts, eds, Balkema, Rotterdam, The Netherlands, 41–50.

Jaeger, C. (1948) Water hammer effects in power conduits. (4 Parts). *CivilEngineering. and Public Works Review*, 23, 74-76, 138-140, 192-194, 244-246.

Joukowsky, N. (1900)Über den hydraulischenStoss in Wasserleitungen.*Memoires de l'academieimperiale de St.-Petersbourg. Classephysico-mathematique*, St. Petersbourg, Russia, 9(5) (in German).

Kita, Y., Adachi, Y. and Hirose, K. (1980)Periodically oscillating turbulent flow in a pipe. *Bulletin JSME*, 23(179), 656–664.

Parmakian, J. (1985) Water column separation in power and pumping plants. *Hydro Review*, 4(2), 85-89.

Pezzinga, G. (1999) Quasi-2D model for unsteady flow in pipe networks. *Journalof Hydraulic Engineering*, ASCE, 125(7), 676–685.

Silva-Araya, W.F., and Chaudhry, M.H. (1997) Computation of energy dissipation in transient flow. *Journalof Hydraulic Engineering*, ASCE, 123(2), 108–115.

Simpson, A.R. (1986) Large water hammer pressures due to column separation in a sloping pipe. PhD thesis, University of Michigan, Ann Arbor, USA.

Simpson, A.R. and Wylie, E.B. (1989) Towards an improved understanding of waterhammer column separation in pipelines. Civil Engineering Transactions 1989, The Institution of Engineers, Australia, CE31(3), 113-120.

Simpson, A.R., and Wylie, E.B. (1991) Large water hammer pressures for column separation in pipelines. *Journal of Hydraulic Engineering*, ASCE, 117(10), 1310-1316.

Shuy, E.B. andApelt, C.J. (1983) Friction effects in unsteady pipe flows. *Pro., 4th Int. Conf. on Pressure Surges (Eds. Stephens, H.S., Jarvis, B., Goodes, D.)*, BHRA, Bath, UK, 147-164.

Vardy, A.E., and Brown, J.M.B. (1996)On turbulent, unsteady, smooth-pipe flow. *Proc., Int. Conf. on Pressure Surges and Fluid Transients*, BHR Group, Harrogate, England, 289-311.

Vardy, A.E. and Hwang, K.L. (1991) A characteristics model of transient frictionin pipes. *Journal of Hydraulic Research*, IAHR , 29(5), 669–684.

Wylie, E.B. (1984) Simulation of vapourous and gaseous cavitation. *Journalof Hydraulic Engineering*, ASME, 106(3), 307-311.

Wylie, E. B., and Streeter, V.L. (1978)*Fluid transients*. McGraw-Hill, New York.

Wylie, E.B. and Streeter, V.L. (1993)*Fluid transients in systems*. Prentice-Hall, Englewood Cliffs, New Jersey.

Zhao, M. andGhidaoui, M.S. (2003) Efficient quasi-two-dimensional model for water hammer Problems. *Journalof Hydraulic Engineering*, ASCE, 129(12), 1007-1013.